CRYOGENIC AND AMBIENT GASEOUS HYDROGEN BLOWDOWN WITH DISCHARGE LINE EFFECTS

Venetsanos A.G.[1*], Giannissi S.[1], Tolias I.[1], Friedrich A.[2], Kuznetsov M.[3]
[1] Environmental Research Laboratory, National Centre for Scientific Research "Demokritos", 15310 Aghia Paraskevi, Attikis, Greece,
[2] Pro-Science GmbH, Parkstrasse 9, Ettlingen, 76275, Germany
[3] Karlsruhe Institute of Technology, 76344, Eggenstein-Leopoldshafen, Germany
*venets@ipta.demokritos.gr

Keywords: Cryogenic hydrogen, choked flow, blowdown, discharge line effects, PIF algorithm

Abstract

The present work performed within the PRESLHY EC-project, presents a simplified 1-d transient modelling methodology to account for discharge line effects during blowdown. The current formulation includes friction, extra resistance, area change, and heat transfer through the discharge line walls, and is able to calculate the mass flow rate and distribution of all physical variables along the discharge line. Choked flow at any time during the transient is calculated using the Possible Impossible Flow (PIF) algorithm. Hydrogen single phase physical properties and vapour-liquid equilibrium are calculated using the Helmholtz Free Energy (HFE) formulation. Homogeneous Equilibrium Mixture (HEM) model is used for two-phase physical properties. Validation is performed against the new experiments with compressed gaseous hydrogen performed at the DISCHA facility in the framework of PRESLHY (200 bar, ambient and cryogenic initial tank temperature 77 K and 4 nozzle diameters 0.5, 1, 2 and 4 mm) and an older experiment at 900 bar, ambient temperature and 2 mm nozzle. Predictions are compared against measured data from the experiments and the relative importance of line heat transfer compared to flow resistance is analysed.

1 INTRODUCTION

Safety analysis of hypothetical accidents in hydrogen applications examines three main phenomena, the release of hydrogen the dispersion of hydrogen (mixing with ambient air) near and further away from the release location and the combustion of hydrogen after potential ignition. In the present work the focus is given on the release phenomena and their transient character.

The transient release (blowdown) from a pressurized gaseous hydrogen tank has been studied both experimentally and theoretically in the past [1,2,3]. Earlier work using nitrogen as a surrogate of hydrogen was reported in [4]. The experimental part of this work performed at the DISCHA facility considered systematic examination of nitrogen blowdown at initial storage pressures in the range 30-200 bars, ambient initial temperatures and 5 nozzle sizes with diameters 0.5,1, 2, 3 and 4 mm.

Earlier modelling work focused on using non-ideal gas properties as well as including transient heat transfer through the tank walls, since the adiabatic tank assumption was shown to lead to tank temperatures much lower than the experimentally recorded. Effects of discharge line were not accounted for explicitly in the abovementioned studies and instead a discharge coefficient was selected to represent this effect and match simulations to experiments.

The present work performed within the PRESLHY EC-project, presents a simplified 1-d transient modelling methodology to account for discharge line effects during blowdown. It is based on the earlier modelling work reported in [5] for steady two-phase releases. The current formulation includes friction, extra resistance (e.g. due to valves or other fittings), area change, and heat transfer through the discharge line walls, and is able to calculate mass flow rate and distribution of all physical variables along the discharge line. Validation is performed against the new experiments with compressed gaseous hydrogen performed at the DISCHA facility in the framework of PRESLHY [6,7] and one of the experiments reported in [2]. The new DISCHA experiments included both ambient and internal cryogenic bulk temperature in the tank.

2 MATHEMATICAL-NUMERICAL FORMULATION

2.1 Conservation equations

Mass and energy conservation equations for the tank (subscript '0') are given below, where ρ, s are the tank averaged density and entropy, V, A the tank free volume and its enclosing surface, $\dot{m}$ the mass flow rate into the discharge line, subscript 'out' referring to conditions at the beginning of the discharge line and $\dot{q}_T$ the heat flux through A:

$$V\frac{d\rho_0}{dt} = -\dot{m} \tag{1}$$

$$V\frac{d\rho_0 s_0}{dt} = -\dot{m}s_{out} + \frac{\dot{q}_0 A_0}{T_0} \tag{2}$$

Mass, momentum and energy conservation equations along the discharge line are given below, where *dx* is the step along the line, $\dot{q}_{in}$ the heat flux at the internal wall, A_{in}, D_{in} the flow cross section and line internal diameter (considered variable along the line), h the enthalpy, f_D the Darcy friction factor and *L* is the length over which the extra resistance factor *K* applies:

$$\rho u = \dot{m}/A_{in} \tag{3}$$

$$\rho u du = -dP - \frac{\rho u^2 dx}{2}\left(\frac{f_D}{D_{in}} + \frac{K}{L}\right) \tag{4}$$

$$\rho u d\left(h + \frac{u^2}{2}\right) = \dot{q}_{in}\frac{4dx}{D_{in}} \tag{5}$$

One-dimensional integral energy conservation equation inside the discharge line walls is given below, where subscripts 'in' and 'ex' refer to the internal and external surface of the discharge line respectively, subscript 'w' refers to wall material, subscript 'amb' refers to ambient conditions, T_w is the thickness averaged wall temperature, a is heat transfer coefficient, and λ, ρ, c_P the wall conductivity, density and specific heat respectively.

$$\rho_w c_{Pw}\left(\frac{D_{ex}^2 - D_{in}^2}{4}\right)\frac{dT_w}{dt} = \dot{q}_{ex}D_{ex} - \dot{q}_{in}D_{in} \tag{6}$$

$$\dot{q}_{ex} = \frac{\lambda_w a_{ex}}{\lambda_w + a_{ex}\Delta D/2}\left(T_{amb} - T_w\right), \quad \dot{q}_{in} = \frac{\lambda_w a_{in}}{\lambda_w + a_{in}\Delta D/2}\left(T_w - T\right) \tag{7}$$

The present mathematical formulation can be characterized as 'quasi-steady', from the fact that although transient equations are used for the tank and piping walls, a steady state formulation is used for the mass, momentum and energy equations along the discharge line. This approach is based on the assumption that the time scale of the flow in the discharge line is much smaller than the time scale of the blow-down and the time scale of pipe wall heat transfer and therefore the flow adapts to a steady state very fast.

2.2 Friction, heat transfer and resistance

Darcy friction factor was calculated from Colebrook's equation for rough walls, where e is the absolute roughness and Re the Reynolds number of the flow:

$$\frac{1}{\sqrt{f_D}} = -2\log_{10}\left(\frac{e/D_{in}}{3.7} + \frac{2.51}{\mathrm{Re}\sqrt{f_D}}\right) \tag{8}$$

Resistance factor for sudden pipe contraction is taken from [8], where A is the flow cross section and subscripts 1, 2 refer to upstream and downstream conditions:

$$K = \frac{1}{2}\left(1 - \frac{A_2}{A_1}\right) \tag{9}$$

Resistance factor for a ball valve was assumed to correspond to an equivalent L/D diameter of 3:

$$K = 3 f_D \tag{10}$$

Internal heat transfer coefficient was calculated using Reynolds analogy:

$$a_{in} = \frac{f_D}{8}\rho u c_P \tag{11}$$

2.3 Numerical considerations

The computational algorithm at each time during a blow-down, starts with calculation of the choked mass flow rate along the line for given tank stagnation conditions. This calculation is performed using the Possible Impossible Flow (PIF) iterative maximization procedure, with inlet pressure as iteration variable. For given inlet pressure, other inlet conditions and mass flow rate are calculated assuming isentropic expansion from the known stagnation conditions, see [9]. With given mass flow rate, discharge line equations (discretized along the line) are solved step by step towards line exit until either non-possible flow is encountered at given step or given mass flow rate is possible throughout the line. If the first condition is reached inlet pressure is increased in the next PIF iteration and the opposite for the second condition. The above PIF procedure is general and once fine line discretization is used near the nozzle exit (minimum cross section) it produces (as output) Mach equal to one at the exit for under-expanded flow.

Solution of the discharge line equations within a given step (dx) along the line is not trivial. The procedure used here is iterative, with the downstream pressure as external iterations variable. For given downstream pressure, first we obtain the other downstream conditions by iteratively solving the energy equation (Fanno line) over temperature or vapour quality and then correct the downstream pressure until the momentum equation (Rayleigh line) is also satisfied. Vapour quality solution is attempted first (assuming saturation temperature). If vapour quality is found beyond the physical range (0.0-1.0) then the flow is in single phase conditions and temperature solution is applied. If the Fanno and Rayleigh lines are found not to intersect then the given mass flow rate is considered as not possible.

Once the choked mass flow rate has been calculated, the new tank density (at the next time) can be calculated from the tank mass equation and the new tank entropy from the tank's energy equation. Other tank stagnation conditions (e.g. temperature, pressure, enthalpy, vapour quality etc.) can be calculated knowing density and entropy. In case the tank stagnation conditions time history is given (e.g. from experiments), the tank mass / energy conservation equations are not used and the numerical problem reduces to performing a series of choked flow calculations for each given time.

Physical properties for normal hydrogen are calculated using the Helmholtz Free Energy based EoS according to [10]. Since physical properties (including pressure) according to this formulation depend on density and temperature, while usually pressure and temperature are given, first we obtain density by iteratively solving the pressure equation for given pressure and temperature and then calculate all other required properties (such as enthalpy, entropy, etc.) explicitly. In case of two-phase conditions HEM model is used for the two-phase physical properties, see [9].

Program execution speed has been highly optimized using Brent's iterative root finding algorithm and Golden section min-maximization algorithm where applicable. Simulation time for PIF algorithm is of the order of few seconds. The simulation time for a full blow-down is order of minutes.

3 RESULTS AND DISCUSSION

3.1 DISCHA experiments at 200 bar

The DISCHA experiments [6, 7] were performed by Pro-Science and KIT within the framework of the PRESLHY project. The experiments investigated transient hydrogen releases from a 2.815 dm³ steel tank through a discharge line with 9 mm ID and a length of 39 cm ending in a nozzle, with diameters 0.5, 1, 2 and 4 mm, see Figure 1. Seven tank stagnation pressures were examined from 5 to 200 bar. Tank stagnation temperatures were either 77 K for the cold tests (tank located within a pool of liquid N_2) or ambient temperature for the warm tests. The experiments included continuous tank temperature and pressure monitoring at high frequency (100 and 200 Hz respectively).

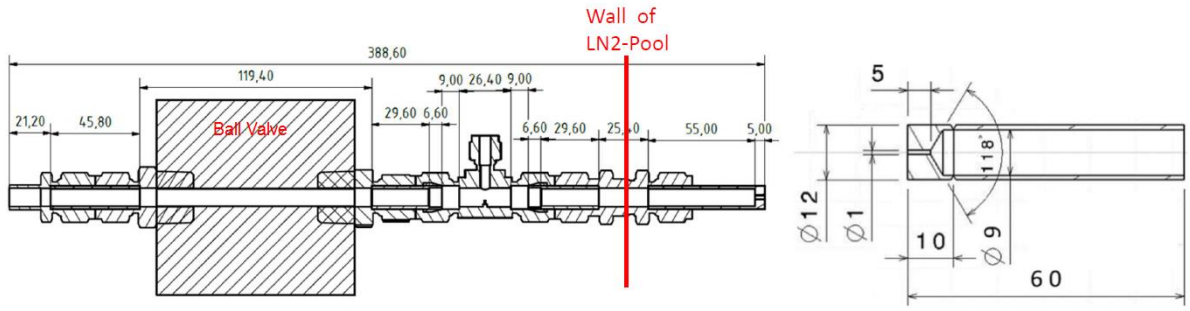

Figure 1. Discharge line (left) and nozzle details (right).

The actual nozzle section of 5 mm length was preceded by additional 5 mm line with diameter linearly changing from 9 mm to nozzle diameter (cone shaped bore). The pipeline material was stainless steel 316, with nominal properties 8000 kg/m^3, 500 J/kg/K and 15 W/m^2/K for density, specific heat and conductivity respectively. The nominal piping thickness was 1.5 mm, while an average thickness of 4.5 mm was estimated (based on weighting) to account for the bolts / nuts shown in Figure 1. The tubing had machined inner surface with relative roughness estimated at 1×10^{-4}. A much larger relative roughness (5×10^{-3}) was used in the calculations for the nozzles, manufactured at KIT's workshop with a drilling process. The ambient heat transfer coefficient was assumed equal to 6 W/m^2/K. For the parts of the discharge line inside the LN_2 bath a constant temperature (77 K) was assumed at the external wall.

In the present work, release calculations were performed for the warm and cold 200 bar cases. Four different modelling approaches were applied: a) Adiabatic tank blow-down without account of the discharge line, b) Real tank stagnation conditions without account of the discharge line, c) Real tank stagnation conditions with adiabatic discharge line and d) Real tank stagnation conditions with non-adiabatic discharge line. In cases (b-d) real tank conditions were taken from the experimental measurements, see Figure 2. It should be noted that model (a) can be found / used within the eLab platform, developed under the NET-Tools EC-project, see https://elab-prod.iket.kit.edu/.

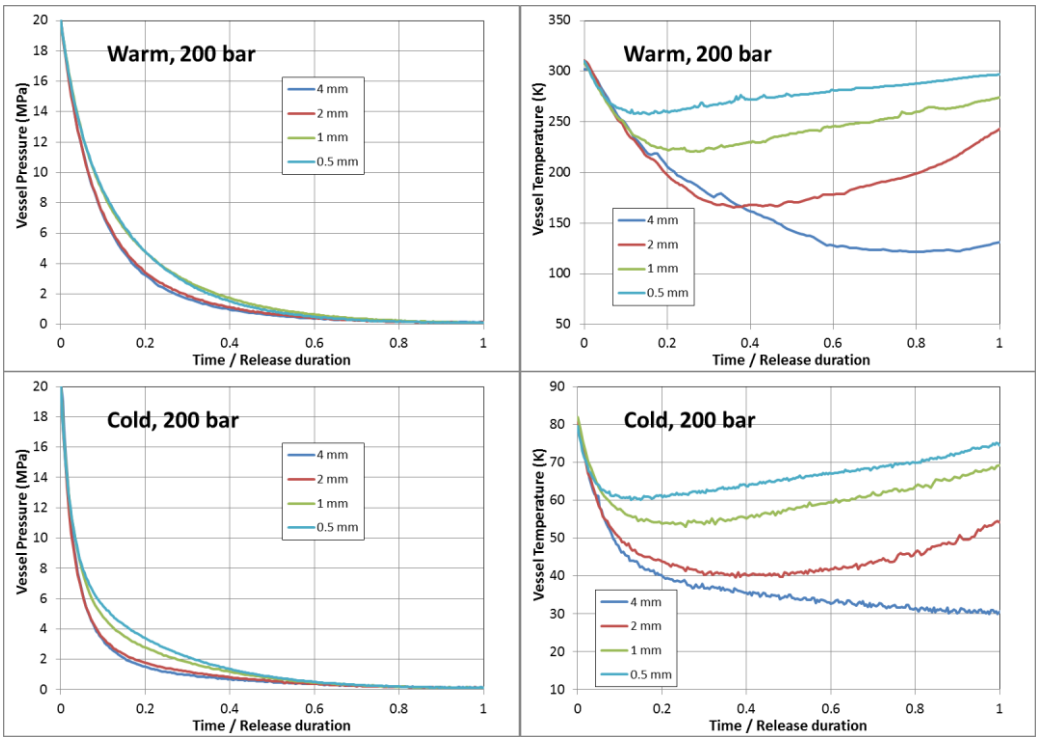

Figure 2. Vessel experimentally recorded stagnation conditions. Estimated release duration: 2.5, 10, 40, 135 s for the warm and 5, 20, 80, 270 s for the cold releases for nozzle diameters 4, 2, 1 and 0.5 mm respectively.

Figure 3 and Figure 4 present the predicted released hydrogen mass time histories compared against the experimental ones for the warm and cold cases respectively. The total hydrogen mass in the tank was approximately 40 g for the warm releases and 140 g for the cold releases. In some cases the model actually predicts more hydrogen mass released than the true mass contained in the tank at the beginning of the transient. This is due to mass flow rate overestimation.

Without account of the discharge line the model assuming an adiabatic tank produces acceptable mass flow rate predictions in most cases considered compared to the experimental data, although this model systematically underestimates both the tank pressure and temperature, as can be observed in Figure 5, this underestimation increasing with decreasing nozzle diameter.

The stagnation conditions during the blowdown of non-insulated tanks are affected by transient heat transfer through the tank walls and, as a result, mass flow rates are expected to be increased compared to the adiabatic tank scenario. This is verified in Figure 3 and Figure 4 which clearly show that when the real tank conditions are used as input to the simulations, the mass flow rates are systematically overestimated if the discharge line is not taken into account.

The general effect of a discharge line is to reduce mass flow rates. Using real tank conditions as input, Figure 3 and Figure 4 show that: a) accounting for an adiabatic discharge line reduces the mass flow rates due to flow resistance and systematically improves the predictions compared to the experimental data b) the discharge line heat transfer (non-adiabatic line assumption) acts as an extra resistance to the flow, i.e. tends to decrease the mass flow rates, which is contrary to the role of the tank heat transfer as mentioned above c) the extra resistance due to line heat transfer is relatively small compared to the flow resistance without including heat transfer effects and d) the extra resistance due to line heat transfer effects increases in cryogenic releases compared to ambient ones.

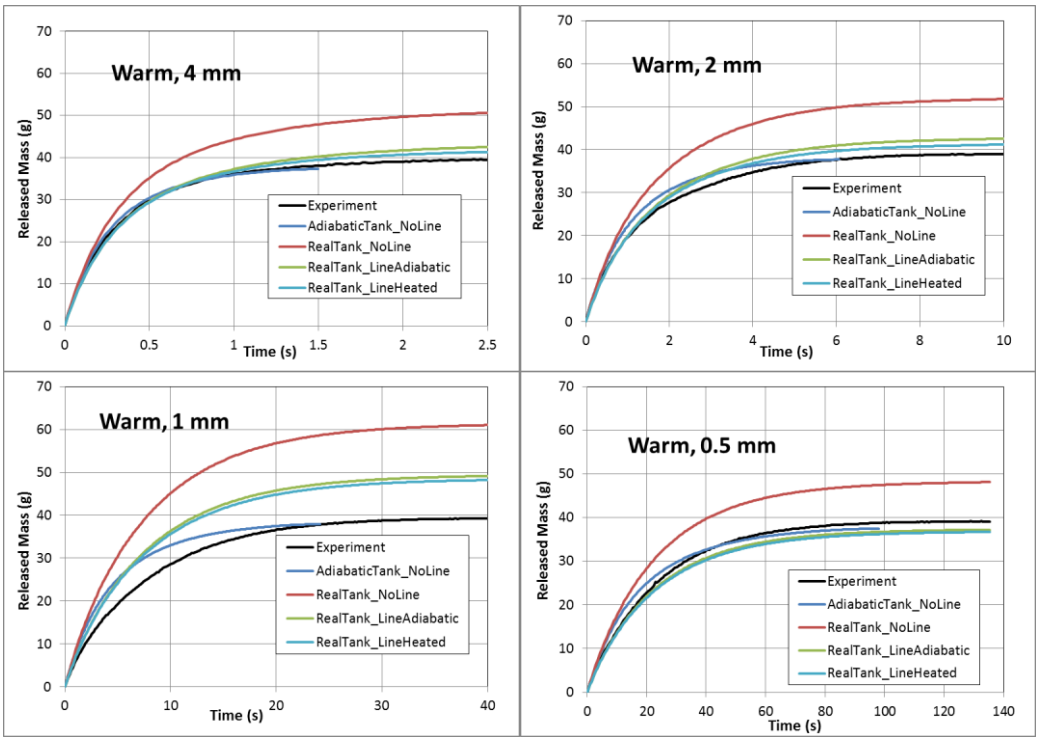

Figure 3. Predicted released hydrogen mass time histories compared against DISCHA experiments at 200 bar for the warm releases.

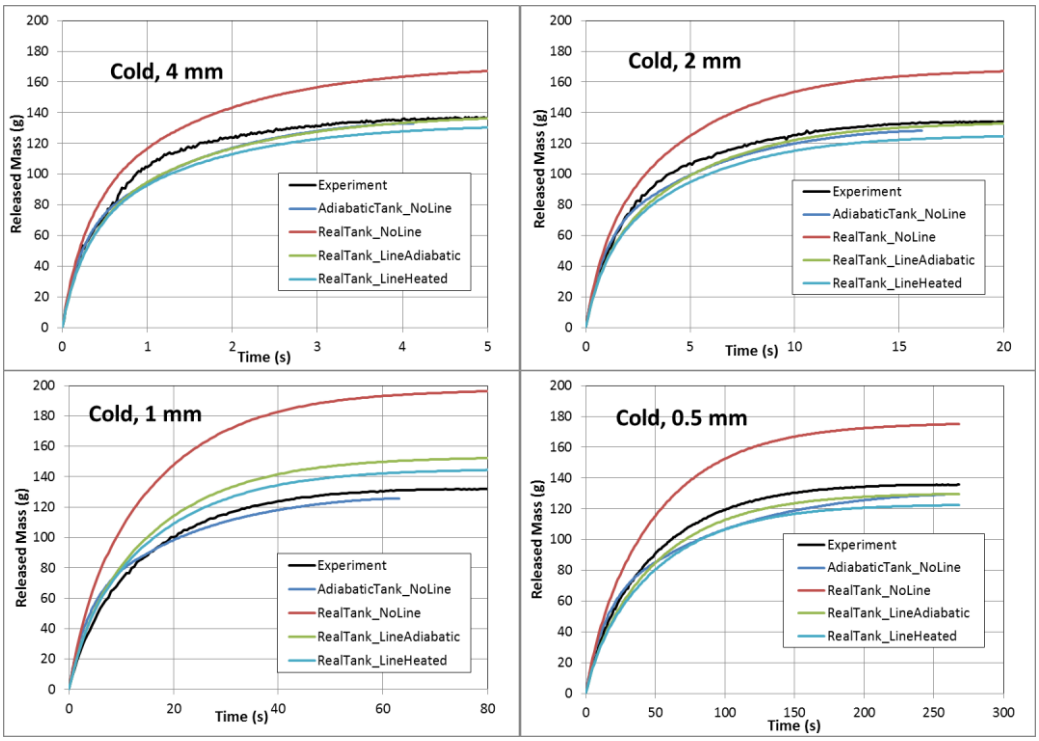

Figure 4. Predicted released hydrogen mass time histories compared against DISCHA experiments at 200 bar for the cold releases.

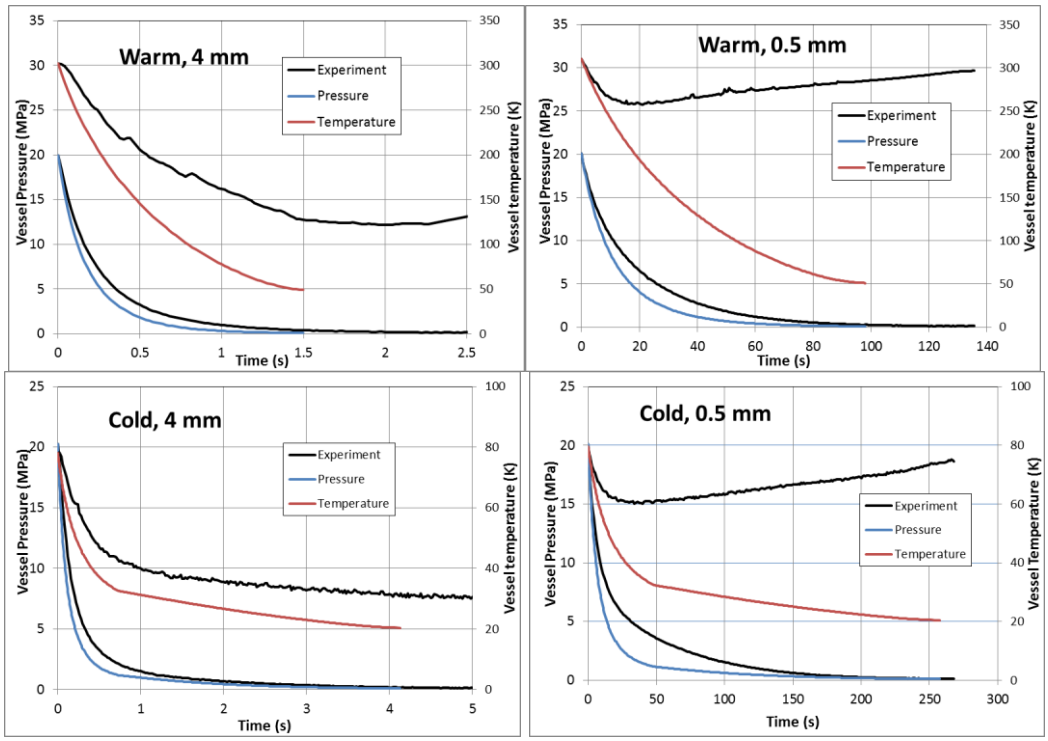

Figure 5. Predicted tank stagnation conditions assuming adiabatic tank and no discharge line compared to experimental.

The simulations including line heat transfer effects were performed with an ambient heat transfer coefficient of 6 W/m^2/K as mentioned above and neglecting any radiation heating of the discharge line that occurs in case of an ignited release or ambient fire. Increasing the heat transfer coefficient to 25 W/m^2/K did not show any noticeable changes in predicted mass flow rates. Significant radiation heating of the nozzle in case of an ignited release might lead to noticeable mass flow rate reduction compared to the un-ignited case and such a phenomenon could be part of a future investigation.

Mass flow rate predictions with models (b, c) were used to express the effect of the discharge line in terms of a "model to model" discharge coefficient. Figure 6 shows that these discharge coefficients a) systematically decrease with nozzle diameter, b) systematically decrease when flow passes from choked to fully expanded and c) are slightly lower for cryogenic releases compared to those at ambient temperature. The abovementioned dependence of discharge coefficient on nozzle diameter was also reported in [4].

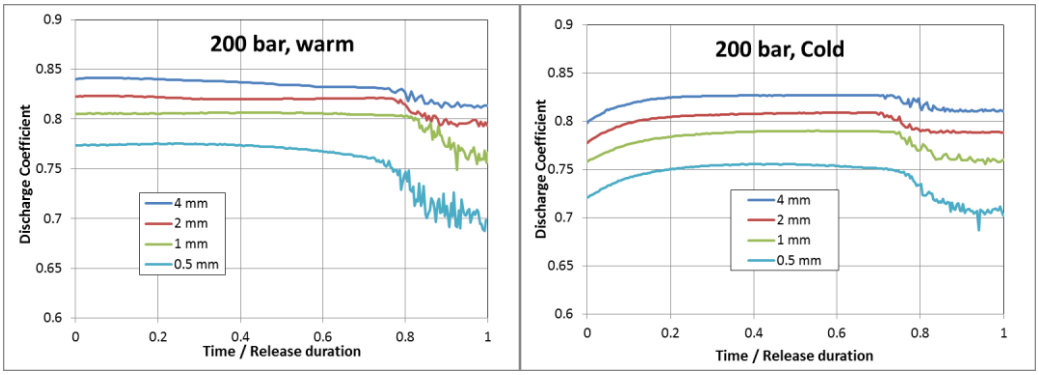

Figure 6. Predicted discharge coefficients for DISCHA experiments. Discharge coefficient is defined here as ratio of predicted mass flow rate with an adiabatic line, to predicted mass flow rate without a line (predictions with given experimental stagnation conditions in both cases).

Figure 7 shows the initial distribution (starting time of the transient) of flow physical variables (pressure, temperature, velocity and Mach number) for the 2 mm nozzle with the model using real tank conditions as input and assuming an adiabatic line. It can be observed that all physical variables are practically constant over the entire line except the 10 mm in length nozzle part where all the significant changes occur. It can also be observed that flow velocities are significantly smaller before the nozzle area compared to the nozzle itself from which it is suggested that any flow resistances before the nozzle section e.g. from the valve are significantly less important in reducing mass flow rate than resistances due to the nozzle. It can finally be observed that at the nozzle exit Mach reaches 1.0 and that pressure gradient at the same location tends to infinity as expected.

A picture similar to Figure 7 was observed in all cases simulated and can be considered as characteristic when the nozzle diameter is less than half that of the preceding discharge line. In case of full bore line rupture on the other hand, the picture is expected significantly different with noticeable changes in the flow occurring all the way from the tank to the line exit.

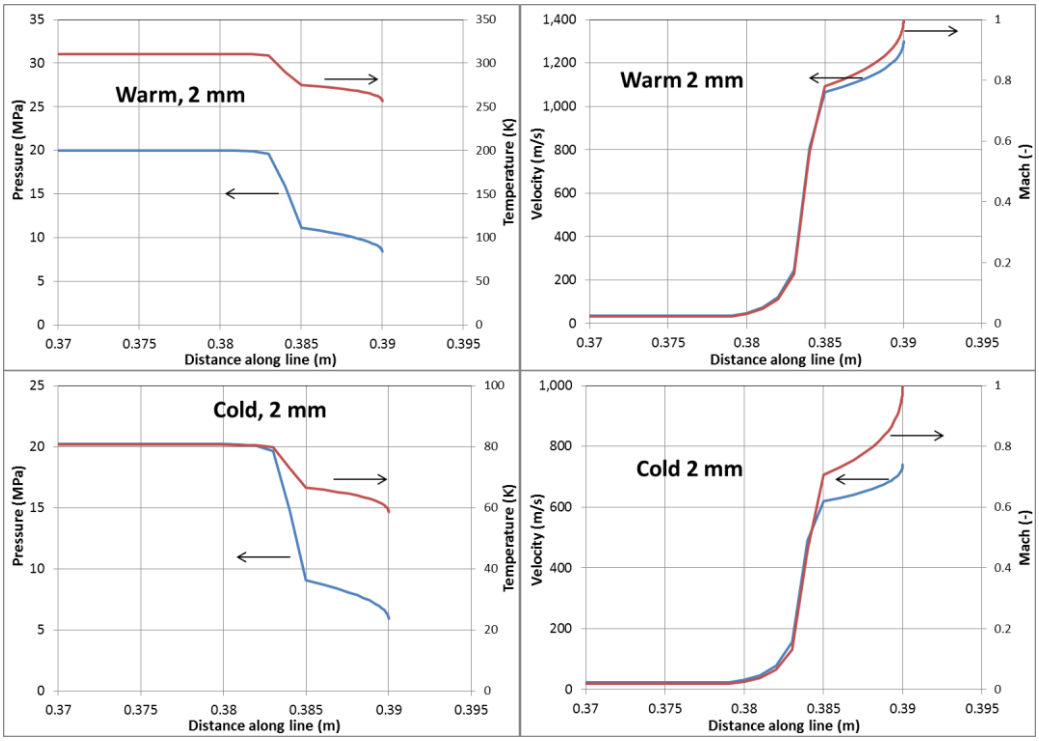

Figure 7. Initial temperature, pressure, velocity and Mach distribution along the discharge line for 2 mm nozzle using model with real tank conditions and an adiabatic line.

Finally, Figure 8 presents predicted conditions at the nozzle exit for the cold release with 4 mm nozzle diameter and all models as function of time. The adiabatic tank model without a discharge line produces two-phase flow at the nozzle exit, the lowest values of exit temperature and velocity and the highest values of exit density. For the model using real tank conditions as input and discharge line heat transfer, the heat flux at the inner wall is observed to reach a maximum of ≈150 kW/m^2 at ≈0.6 seconds before starting to drop and temperatures are observed to increase with respect to the adiabatic discharge line case. It should be noted that if steady state heat transfer is used (instead of transient heat transfer), i.e. equation (6) without the transient term, then the resulting heat flux would be only ≈3 kW/m^2 remaining nearly constant during the blow-down and therefore this case would be practically equivalent to assuming an adiabatic line.

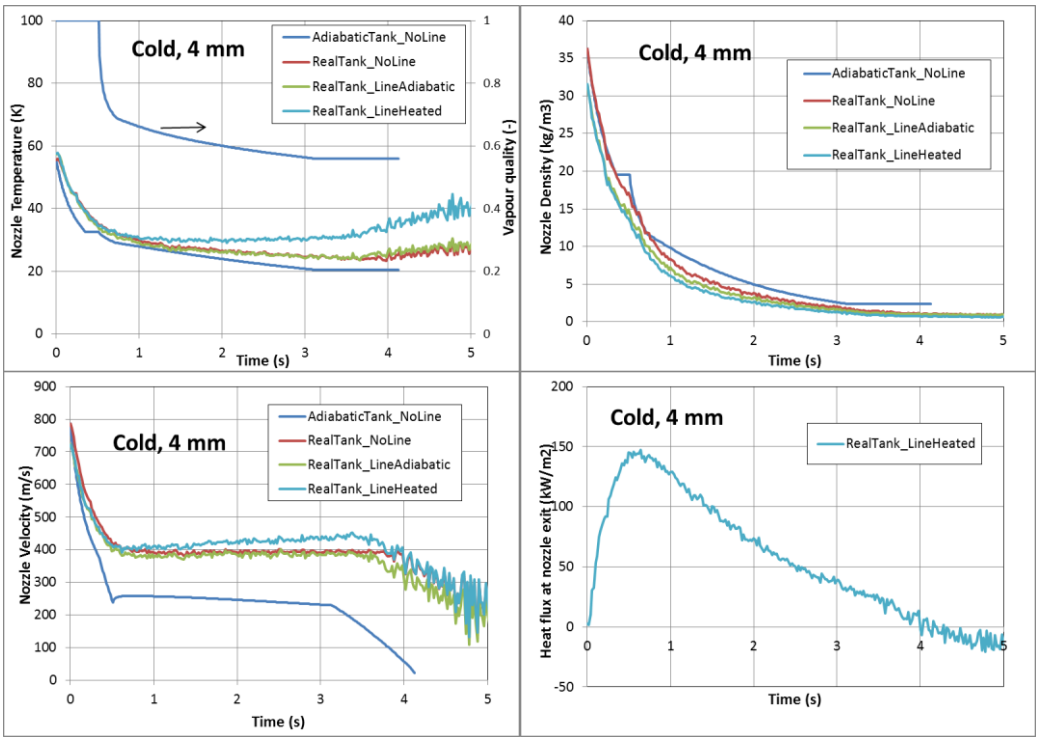

Figure 8. Predicted conditions at the nozzle exit for cold release, 4 mm nozzle.

3.2 INERIS experiment at 900 bar

The INERIS experiments [2] were performed within the French national project DRIVE and the European project HyPER. The selected test was a hydrogen blow-down release from a 25 dm³ type-IV reservoir at 900 bar and ambient temperature, through a 10 m line with 10mm ID ending to a 2 mm diameter nozzle. A nozzle arrangement similar to the DISCHA experiments was assumed for the simulations. Figure 9 shows predicted mass flow rate and corresponding released mass time histories. The observed behaviour of the models is similar to the one described above for the DISCHA hydrogen tests.

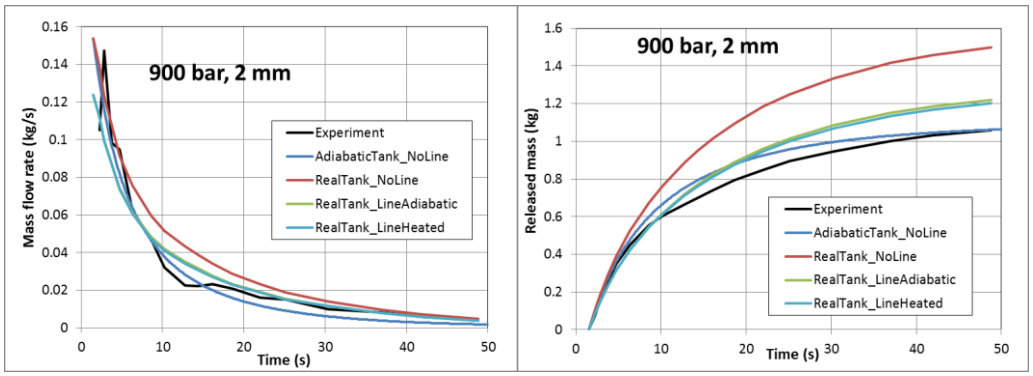

Figure 9. Predicted mass flow rate and released mass time history compared against INERIS experiment.

4 CONCLUSIONS

A simplified 1-d transient modelling methodology was developed to account for discharge line effects during blowdown and validated against hydrogen transient release experiments with 200 bar, ambient or cryogenic temperature (77 K) initial stagnation conditions and 4 nozzle diameters (0.5, 1, 2, 4 mm) and a hydrogen release experiment with 900 bar, ambient temperature and 2 mm nozzle. It was found that:

- Without account of the discharge line:
    - The transient adiabatic tank model (without discharge coefficient) produces released hydrogen mass histories in acceptable agreement to the experiments in most cases considered, although this model systematically underestimates both tank pressure and temperature.
    - When experimental tank stagnation conditions are used as model input throughout the transient, released hydrogen mass histories are systematically overestimated without a discharge coefficient.
- With account of the discharge line and experimental tank stagnation conditions as input:
    - Mass flow rates are reduced and released mass histories are in much better agreement to experiments.
    - Discharge line heat transfer acts as an extra resistance to the flow, which is contrary to the role of tank heat transfer, i.e. to increase mass flow rates. This extra resistance is relatively small compared to the flow resistance without including heat transfer effects and increases in cryogenic releases compared to ambient ones.
    - Predicted "model to model" discharge coefficients were found to decrease with nozzle diameter, decrease when flow passes from choked to fully expanded and generally be slightly lower for cryogenic releases compared to those at ambient temperature.
    - When the nozzle diameter is less than half that of the preceding discharge line then all the significant changes in the flow occur within the nozzle section. In case of full bore line rupture on the other hand, noticeable changes in the flow occurring all the way from the tank to the line exit are expected.

5 ACKNOWLEDGEMENTS

The research leading to these results was financially supported by the PRESLHY project, which has received funding from the Fuel Cells and Hydrogen 2 Joint Undertaking under the European Union's Horizon 2020 research and innovation program under grant agreement No 779613. This Joint Undertaking receives support from the European Union's Horizon 2020 research and innovation programme, Hydrogen Europe and Hydrogen Europe research.

6 REFERENCES

1 Schefer R.W., Houf W.G., Williams T.C., Bourne B., Colton J., Characterization of high-pressure, underexpanded hydrogen-jet flames, Int. J. Hydrogen Energy, 32 (2007) 2081-2093.

2. Proust C., Jamois D., Studer E., High pressure hydrogen fires, Int. J. Hydrogen Energy, 36 (2011) 2367-2373.

3 Dadashzadeh M., Makarov D., Kashkarov S., Molkov V., Non-adiabatic under-expanded jet theory for bowdown and fire resistance rating of hydrogen tank, 8th Int. Conf. on Hydrogen Safety, 24-26 Sept. 2019, Adelaide, Australia.

4 Kuznetsov M., Pariset S., Friedrich A., Stern G., Travis J., Jordan T., Experimental investigation of non-ideality and non-adiabatic effects under high pressure releases, Int. J. Hydrogen Energy, 40 (2015) 16398-16407.

5 Venetsanos A.G., Choked two-phase flow with account of discharge line effects, 8th Int. Conf. on Hydrogen Safety, 24-26 Sept. 2019a, Adelaide, Australia.

6. Friedrich A., Veser A., Jordan T., Summary of experiment series E3.1 (Discharge) results – part A high pressure, PRESLHY deliverable D3.4 (D21), 2019.

7. Veser A., Friedrich A., Kuznetsov M., Jordan T., Kotchourko N., Hydrogen blowdown release experiments at different temperatures in the DISCHA-facility, 9th Int. Conf. on Hydrogen Safety, 21-23 Sept. 2021, Edinburgh, UK.

8. Idel'chik I.E., Handbook of Hydraulic resistance, Coefficients of local resistance and of friction, 1966, pp. 517.
9. Venetsanos A.G., Homogeneous non-equilibrium two-phase choked flow modelling, Int. J. Hydrogen Energy, 43 (2018) 22715-22726.
10. Leachman J.W., Jacobsen R.T., Penoncello S.G., Lemmon E.W., Fundamental Equations of State for Parahydrogen, Normal Hydrogen, and Orthohydrogen, J. Phys. Chem. Ref. Data, 38 (2009) 721-748.